Title	Growth and Microstructure of Epitaxial Ti3SiC2 Contact Layers on SiC
Author(s)	Tsukimoto, Susumu; Ito, Kazuhiro; Wang, Zhongchang; Saito, Mitsuhiro; Ikuhara, Yuichi; Murakami, Masanori
Citation	MATERIALS TRANSACTIONS (2009), 50(5): 1071-1075
Issue Date	2009-05
URL	http://hdl.handle.net/2433/109943
Right	Copyright (c) 2009 The Japan Institute of Metals
Type	Journal Article
Textversion	publisher

Materials Transactions, Vol. 50, No. 5 (2009) pp. 1071 to 1075
Special Issue on Nano-Materials Science for Atomic Scale Modification

Growth and Microstructure of Epitaxial Ti_3SiC_2 Contact Layers on SiC

Susumu Tsukimoto[1], Kazuhiro Ito[2], Zhongchang Wang[1], Mitsuhiro Saito[1], Yuichi Ikuhara[1,3] and Masanori Murakami[4]

[1]*World Premier International Research Center, Advanced Institute for Materials Research (WPI-AIMR), Tohoku University, Sendai 980-8577, Japan*
[2]*Department of Materials Science and Engineering, Kyoto University, Kyoto 606-8501, Japan*
[3]*Institute of Engineering Innovation, The University of Tokyo, Tokyo 113-8656, Japan*
[4]*The Ritsumeikan Trust, Kyoto 604-8520, Japan*

Growth and microstructure of ternary Ti_3SiC_2 compound layers on 4H-SiC, which play am important role in formation of TiAl-based ohmic contacts to p-type SiC, were investigated in this study. The Ti_3SiC_2 layer was fabricated by deposition of Ti/Al contacts (where a slash "/" indicates the deposition sequence) on the 4H-SiC(0001) substrate and subsequent rapid thermal anneal at 1000°C in ultra high vacuum. After annealing, reaction products and microstructure of the Ti_3SiC_2 layer were investigated by X ray diffraction analysis and transmission electron microscopy observations in order to understand the growth processes of the Ti_3SiC_2 layer and determination of the Ti_3SiC_2/4H-SiC interface structure. The Ti_3SiC_2 layers with hexagonal plate shape were observed to grow epitaxially on the SiC(0001) surface by anisotropic lateral growth process. The interface was found to have a hetero-epitaxial orientation relationship of $(0001)_{TSC}//(0001)_S$ and $[0\bar{1}10]_{TSC}//[0\bar{1}10]_S$ where TSC and S represent Ti_3SiC_2 and 4H-SiC, respectively, and have well-defined ledge-terrace structures with low density of misfit dislocations due to an extremely low lattice mismatch of 0.4% between Ti_3SiC_2 and 4H-SiC. [doi:10.2320/matertrans.MC200831]

(Received November 25, 2008; Accepted January 26, 2009; Published March 11, 2009)

Keywords: *Ti_3SiC_2, 4H-SiC, TiAl, lateral growth, interface*

1. Introduction

Silicon carbide (SiC) is one of the most attractive compound semiconductors for next generation high-power electronic devices operated at high temperature because of its excellent intrinsic properties such as a wide band gap, a high thermal conductivity, a high electric field breakdown strength, and a high saturation electron velocity.[1–4] However, development of low resistance ohmic contacts to p-type SiC is a key technology issue in the fabrication of highly reliable and high performance devices.[5,6] Crofton *et al.*[7] found that binary Ti-Al alloy contacts yielded very low contact resistance to p-type SiC after annealing at temperatures higher than 1000°C. After that, extensive investigations for improvement of the binary Ti-Al contacts and development of other p-type ohmic contact materials have been carried out by various authors.[8–13]

Microstructures of the TiAl-based ohmic contacts were investigated by transmission electron microscopy (TEM) observations, and these contacts were found to grow Ti_3SiC_2 on the SiC surface at high temperature of 1000°C in high vacuum.[14–16] From TEM observations and electrical properties, it is concluded that formation of the Ti_3SiC_2 layers was required to achieve excellent ohmic properties for p-type SiC, resulting in reduction of height of Schottky barrier formed at the metal/SiC interface and enhancement of carrier transportation across the contact interfaces.[14,17] However, the role of the Ti_3SiC_2/SiC interface on mechanism by which the Schottky barrier height reduce has not been well clarified yet. In addition, the atomic structure at/near the Ti_3SiC_2/SiC interface, which is important to elucidate the carrier transport mechanism, also has not been investigated extensively and understood yet as well as the growth of the Ti_3SiC_2 compound on SiC has. The primary purpose of the present study is to understand growth process and formation of the Ti_3SiC_2 compound in the conventional Ti/Al ohmic contacts on SiC annealed at high temperature in order to obtain a clue to reduce the Schottky barrier height. For this purpose, the microstructure at the contact materials/SiC interfaces after isothermal annealing at 1000°C for various storage times are correlated.

2. Experimental Procedures

4H-SiC epitaxial layers (5 μm-thick) doped with aluminum which were grown on undoped 4H-SiC wafers by chemical vapor deposition (manufactured by Cree Research, Inc.) were used as the substrates. Here, the 4H-SiC substrates had 8°-off Si-terminated (0001) surfaces inclined toward a $[\bar{2}110]$ direction because only 4H-type structure of SiC with polymorph (e.g. 3C, 4H, 6H, 15R etc.) was controllable by lateral growth of the epitaxial layers parallel to (0001)-oriented surface. After chemical cleaning of the substrate surface, a 10 nm-thick sacrificial oxide (SiO_x) layer was grown on the SiC substrate by dry-oxidation at 1150°C for 60 min. The substrates were cleaned by dipping in 5% diluted hydrofluoric acid solution and rinsing in deionized water prior to deposition of contact materials. Then, Ti and Al stacking layers with high purities were deposited sequentially on the substrate in a high vacuum chamber where the base pressure was below 5×10^{-6} Pa. The thicknesses of the Ti and Al layers investigated in this study are 100 nm and 380 nm, respectively, and these layer thicknesses were chosen to give the average composition of the Ti(20 at%) and Al(80 at%), where the layer thicknesses were measured by a quartz oscillator during deposition. The reasons to choose this average composition was that aluminum rich (more than 75 at%) in TiAl contacts were empirically found to be essential to yield low contact resistance, resulting from formation of the Ti_3SiC_2 compound layers.[18] After deposit-

ing, the binary Ti/Al contact layers were annealed at 1000°C for various storage times of 2, 4 and 6 min in an ultra-high vacuum chamber where the vacuum pressure was below 1×10^{-7} Pa.

The surface morphology of the Ti/Al contact layers on 4H-SiC after annealing was observed using a JEOL JSM-6060 scanning electron microscope (SEM). Microstructural analysis and identification of the Ti_3SiC_2 layers at the contact layers/4H-SiC interfaces after annealing was performed using X-ray diffraction (XRD) and cross-sectional TEM. For XRD analysis, Rigaku RINT-2500 with Cu $K\alpha$ radiation operated at 30 kV and 100 mA was used. In particular, the interfacial structures and an orientation relationship between the contact layers and the 4H-SiC substrates were characterized by cross-sectional high-resolution TEM observations and selected area diffraction pattern (SADP) analysis, respectively, using a JEOL JEM-4000EX electron microscope operated at an accelerating voltage of 400 kV, where the point-to-point resolution of this microscope was approximately 0.17 nm. Thin foil specimens for the TEM observations were prepared by the standard procedures; cutting, gluing, mechanical grinding, dimple polishing, and argon ion sputter thinning techniques.

3. Results and Discussion

3.1 Formation of ternary Ti_3SiC_2 compound on SiC

XRD analysis was performed to characterize the microstructures of the Ti/Al contacts deposited on the SiC substrates after annealing in order to understand growth and formation of the Ti_3SiC_2 compounds. Figures 1 show XRD profiles obtained from the Ti(100 nm)/Al(380 nm) contact layers before and after annealing at 1000°C. Before annealing, the metallic Ti and Al are detected as shown in Fig. 1(a). It is noted that the intensity of the peak diffracted from Ti is very weak because the grain sizes of the as-deposited Ti layer are much smaller than those of the Al layer. After annealing for 2 min, binary Al_3Ti, Al_4C_3 and ternary Ti_3SiC_2 compounds, which were formed by interfacial chemical reaction, are detected by XRD analysis in addition to unreacted Al (Fig. 1(b)). Note that an amount of the Al_4C_3 compounds is quite small because the intensity of the peak diffracted from Al_4C_3 is very weak. After annealing for 4 min (Fig. 1(c)), it is observed that the Ti_3SiC_2 peak intensities increase and the Al_3Ti peak intensities decrease, although the intensities of the peaks diffracted from other compounds do not change significantly. The peaks diffracted from Al_3Ti disappear after annealing for 6 min as shown in Fig. 1(d). From this XRD analysis, only the Ti_3SiC_2 peaks diffracted from (000*l*) diffraction planes of a hexagonal structure are observed. This result indicates that the Ti_3SiC_2 layer, which is a dominant phase formed by reacting of the Ti-80%Al contact and SiC at 1000°C, has a strong (0001)-oriented texture or hetero-epitaxy on the SiC substrate.

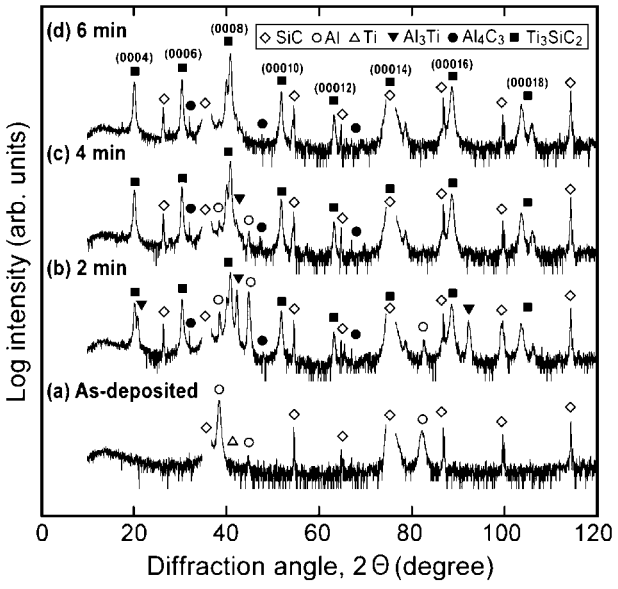

Fig. 1 XRD profiles obtained from the Ti(100 nm)/Al(380 nm) contact layers (a) before and after annealing at 1000°C with various storage times of (b) 2 min, (c) 4 min, and (d) 6 min.

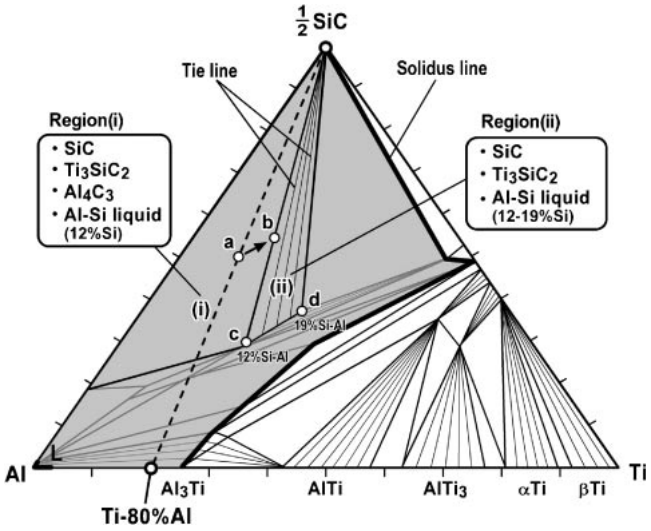

Fig. 2 Isothermal section of a pseudoternary phase diagram of Al-Ti-SiC system at 1000°C proposed by Viala *et al.*[19]

Figure 2 shows an isothermal section of the pseudoternary phase diagram of Al-Ti-SiC system at 1000°C constructed by Viala *et al.*[19] based on their experimental measurements of Al-Ti-Si-C quaternary system, where a grey region indicates the existence of binary AlSi-based liquid phases, and thick and fine lines indicates sub-solidus lines and tie-lines, respectively. It is noted that the liquidus line would lie at near the composition region of pure Al as denoted by a symbol *L* in Fig. 2. Based on this phase diagram, the liquid phase is predicted to form when the concentration of Al is more than 75 at% in the Ti/Al contacts at 1000°C. In general, both the solutes and solvents have high diffusitivity in liquid, thus the liquid phase has high reactivity to solid (substrate) and the reaction products are easily formed at elevated temperatures. Formation of the liquid is believed to play an important role in formation of the TiAl-based contact by rapid thermal anneal process. Here, the effective average composition of the present reaction system, which react Ti-80%Al and SiC, can assume to be at the point *a* within region (i) in the diagram. In this region, four phases of SiC, Al_4C_3, Ti_3SiC_2 and liquid with a composition of Al-12%Si (which is a eutectic composition of Al-Si binary alloy) is predicted to

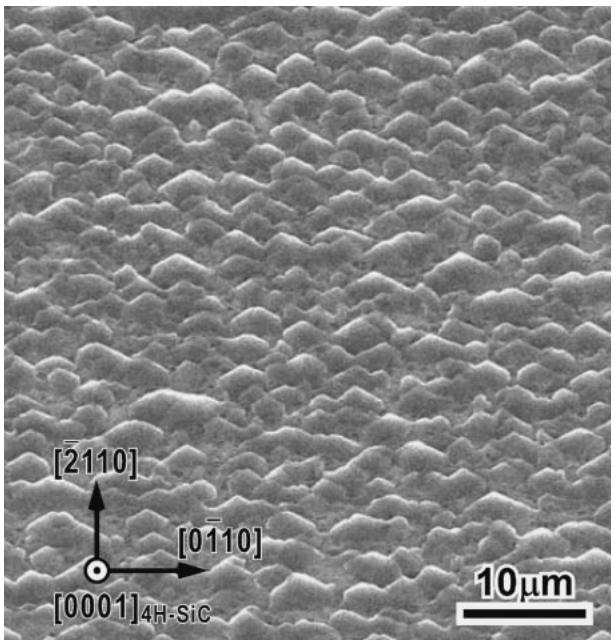

Fig. 3 A plan-view SEM image of the Ti/Al contact layers deposited on SiC after annealing at 1000°C for 6 min.

be invariant and coexist in equilibrium. This prediction is consistent with the XRD results obtained from samples annealed at 1000°C for short storage times of 2 and 4 min as shown in Fig. 1(b) and (c), although a small amount of Al_3Ti and Al did not react completely with SiC and remained at this stage. After annealing for 6 min (as indicated in Fig. 1(d)), disappearance of these unreacted Al_3Ti and Al is occurred due to additional reaction to form the carbides (Ti_3SiC_2 and a small amount of Al_4C_3) and evaporation of the Al-Si liquid phase with a high vapor pressure during annealing in ultra high vacuum. Thus, the average composition of the reaction system seems to shift toward Al-poor one (region (ii)) as indicated by an arrow and reach to the point *b* after annealing. In the region (ii), three phases of SiC, Ti_3SiC_2 and Al-Si liquid with the Si concentrations varied from 12% (at the point *c*) to 19% (at the point *d*) are coexisted and their volume will be constituted by an array of tie-lines. However, it is not straightforward to control the compounds formed by rapid thermal annealing process because of occurrence of non-equilibrium phenomena such as evaporation of the liquid phases in this reaction system. This would be a reason why the TiAl-based contacts have been fabricated empirically without guidelines for designing the materials.

3.2 Growth and microstructure of Ti_3SiC_2 layers on SiC

In order to characterize the surface morphology of the Ti/Al contact layer after annealing, SEM observation was employed. Figure 3 shows a plan-view SEM image from the Ti/Al contact layer after annealing at 1000°C for 6 min. The surface is observed to have uniformly scale-shaped contrast with hexagonal facet although the surface roughness after annealing was aggravated in comparison with that before annealing (not shown here). Using a stylus surface profiler, the maximum typical roughness was measured to be about 1 μm. The surface facet planes are found to form parallel to $\langle\bar{2}110\rangle$ directions on the SiC(0001) substrate surface. The hillocks on the surface due to formation of residual Al-based liquid droplet, forming after annealing at temperatures lower than 800°C, is not observed. This surface morphology results from evaporation of the liquid phases with low melting points and high vapor pressures during annealing at high temperatures in ultra high vacuum as described in the previous section.

Figure 4(a) shows a cross-sectional bright-field TEM micrograph of a typical region in the Ti/Al contact formed on 4H-SiC after annealing at 1000°C for 6 min. The incident electron beam is along the [0$\bar{1}$10] direction of 4H-SiC, which is parallel to the axis of inclination of the 8°-off SiC (0001) surface. The ternary Ti_3SiC_2 compound layer forms plate-shaped layer with faceted surfaces. A selected area diffraction pattern at the contact/SiC interface is shown in Fig. 4(b), where the arrays of the diffraction spots from the Ti_3SiC_2 layer (dotted lines) and 4H-SiC (solid lines) are shown. The Ti_3SiC_2 layer was found to have an epitaxial orientation relationship with the 4H-SiC substrate:

$$(0001)_{TSC}//(0001)_S \text{ and } [0\bar{1}10]_{TSC}//[0\bar{1}10]_S$$

where TSC and S represent Ti_3SiC_2 and 4H-SiC, respectively. The result of the present TEM investigations is in good agreement with that of the XRD analysis. Both the 4H-SiC ($P6_3/mc$; a = 0.307 nm, c = 1.005 nm)[20] and Ti_3SiC_2 ($P6_3/mmc$; a = 0.306 nm, c = 1.763 nm)[21] have hexagonal crystal unit cells. The lattice mismatch between the basal planes of Ti_3SiC_2 and 4H-SiC across the interface is extremely small and approximately 0.4%. The thickness of the Ti_3SiC_2 layer is not uniform and ranges to 300 nm. The total area of the SiC surface is covered by the Ti_3SiC_2 layers, meaning that no other compound or reaction layers make direct contact with the SiC surface. In addition, the Ti_3SiC_2/SiC interface is observed to have a sawtooth-shaped facet structure as well as the Ti_3SiC_2 surface is. The (0001)-oriented surface of the Ti_3SiC_2 layer is also inclined by 8 degrees toward the substrate surface as shown in Fig. 4(a). This indicates that the surface morphology of the Ti_3SiC_2 layers has a strong influence on the surface orientation of the SiC substrate. Consequently, the scale-shaped surface and interface morphologies is found to originate from growth process and formation of hetero-epitaxial Ti_3SiC_2 layers on the 8°-inclined SiC(0001) substrate surface based on SEM and TEM observations.

Figure 5 shows a cross-sectional high resolution TEM (HRTEM) image of the interface between the Ti_3SiC_2 layer and the 4H-SiC substrate, which is taken along the SiC[$\bar{2}$110] zone axis. It is observed that lattice fringes run parallel to the interface in both the Ti_3SiC_2 layer and the SiC substrate. As for the interface morphology, no contamination or second phase layers were observed, and the Ti_3SiC_2 layer makes direct contact with the SiC substrate. The interface has (0001)-oriented terraces and ledges as marked by letters T_i ($i = 1, 2, 3, 4$) and L_j ($j = 1, 2, 3$) in Fig. 5, respectively. The morphology of the terraces is observed to be atomically flat and abrupt. On the other hand, the ledge heights are found to be well-defined and $n \times$ (a half unit cell height of 4H-SiC: 0.5 nm) where n represents the integer, e.g., $n = 11$ for L_1, $n = 2$ for L_2, and $n = 1$ for L_3. This unique interface morphology is caused by chemical reaction of Ti/Al and SiC,

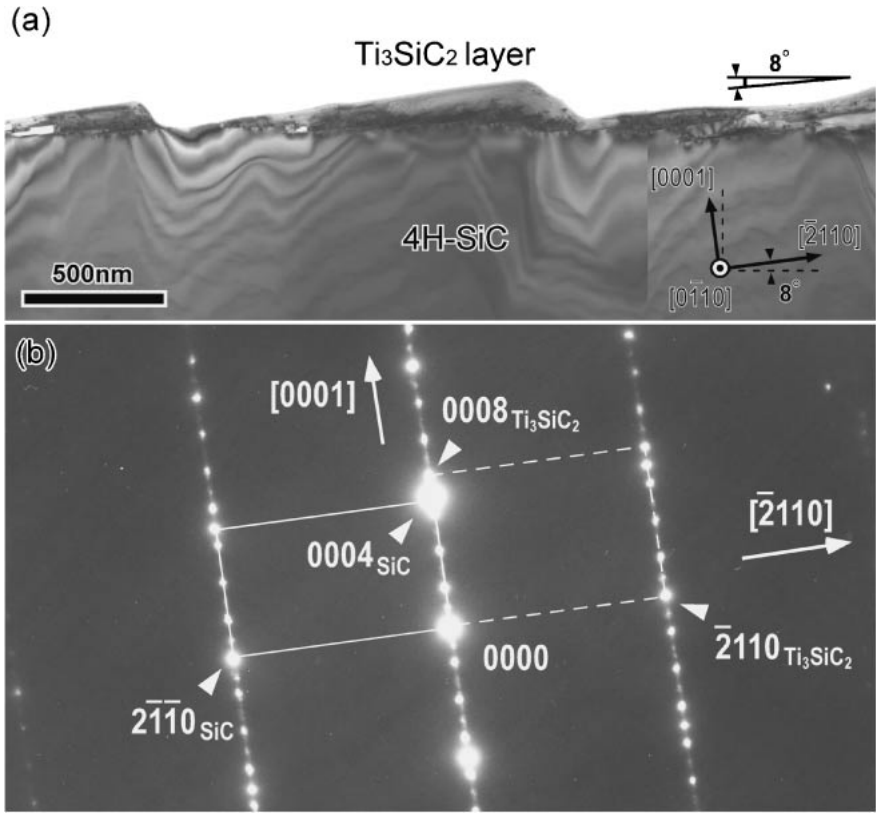

Fig. 4 (a) A cross-sectional bright-field TEM micrograph of a typical region in the Ti/Al contact formed on 4H-SiC after annealing at 1000°C for 6 min, and (b) a selected area diffraction pattern at the contact/SiC interface.

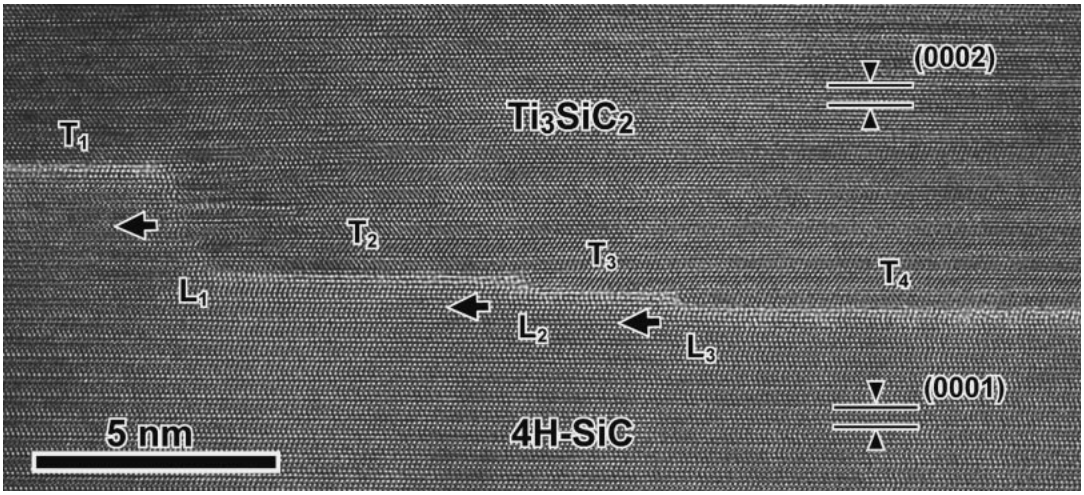

Fig. 5 A cross-sectional HRTEM micrograph of the interface between the Ti_3SiC_2 layer and the 4H-SiC substrate, which is taken along the SiC[$\bar{2}$110] zone axis.

and anisotropic lateral growth of the epitaxial Ti_3SiC_2 layers along the directions parallel to SiC(0001) as indicated by arrows in Fig. 5. A very small number of misfit dislocations were observed at the interface due to the small lattice mismatch between the Ti_3SiC_2 and the 4H-SiC substrate as described above. Figures 6 show a cross-sectional HRTEM micrograph magnified the terrace region (T_4 in Fig. 5) and a schematic projection of atomic structure at the Ti_3SiC_2/4H-SiC interface where the unit cell of Ti_3SiC_2 and 4H-SiC are outlined by rectangle lines. It is noted that the stacking Si-C bilayer marked by termination A of the 4H-SiC substrate surface is observed to make direct contact to Ti_3SiC_2 at the interface. This is in good agreement with the result reported by Kimoto *et al.* that the termination surfaces of the A and C bilayers with crystallographically equivalent relation are energetically much stable than that of the B bilayer in 4H-SiC.[22] From the HRTEM result, the high stability of the termination surfaces A and C in SiC may result in formation of well-defined ledge structure at the Ti_3SiC_2/4H-SiC interfaces as shown in Fig. 5. In addition, it is apparent that Si monolayer in Ti_3SiC_2 with layer structure makes direct bond with Si-terminated layer of 4H-SiC(0001) at the

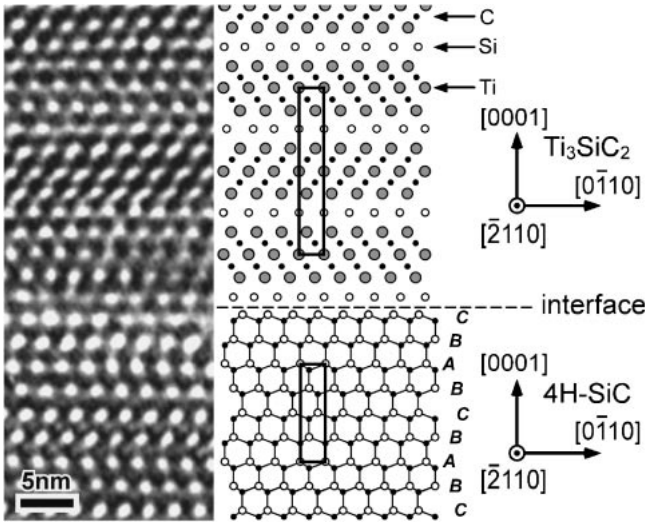

Fig. 6 A cross-sectional HRTEM micrograph magnified the terrace region (T_4) at the Ti_3SiC_2/4H-SiC interface in Fig. 5 and a schematic projection of atomic structure at the interface where the unit cell of Ti_3SiC_2 and 4H-SiC are outlined by rectangle lines.

interface. The Si-Si bonding seen intuitively from the present HRTEM image has been suggested by first-principles calculations to be of covalent character. In addition, calculation results (not shown here) also show that the Si-Si interface has smaller adhesion energy compared to other possible interfaces, which indicates that this interface is relatively weak. The strongest interface predicted by the calculations is the Si-C-Si interface (i.e. the Si-Si interface with introduction of a carbon monolayer). The Si-C-Si interface is predicted to be of mixed covalent-ionic character, have larger charge transfer, and able to realize the formation of ohmic contact. However, it is not straightforward to identify the presence of the C monolayer based on the conventional HRTEM observation technique. Further investigation by combing first-principles modeling with quantitative structure characterization of Z-contrast imaging and spectroscopic analysis (with aberration-corrected scanning transmission electron microscope (STEM)) is required in determining the interface atomic-scale structure and elucidating the formation mechanism of the Ti_3SiC_2 ohmic contacts for p-type SiC.

4. Conclusion

In order to understand chemical reaction processes and growth of ternary Ti_3SiC_2 compounds fabricated by annealing Ti(100 nm)/Al(300 nm) [total composition: Ti-80%Al] contacts deposited on the 4H-SiC(0001) substrate at high temperature of 1000°C, the microstructures were investigated by XRD analysis and TEM/HRTEM observations. From the XRD analysis, the Ti_3SiC_2 compound was found to be a dominant phase formed by reacting of the Ti-80%Al contact and SiC at 1000°C, which was in good agreement with prediction of chemical reaction process and products formed during annealing based on thermodynamics (equilibrium phase diagram). The cross-sectional TEM observations revealed that the Ti_3SiC_2 layers formed by anisotropic lateral growth made direct contact to the SiC substrate surface, and the Ti_3SiC_2 layers had a hetero-epitaxial relationship with the SiC substrates as follows:

$$(0001)[0\bar{1}10]_{TSC}//(0001)[0\bar{1}10]_{S} \quad (\text{TSC: } Ti_3SiC_2, \text{ S: SiC}).$$

Atomically flat terraces and ledges with well-defined heights multiplied about 0.5 nm, which is a half unit cell height of 4H-SiC(0001), were observed at the interfaces between Ti_3SiC_2 and SiC. Although it seems that the Si monolayer in Ti_3SiC_2 with layer structure is bonded to the Si-terminated layer of SiC(0001) at the interface, further investigations combined theoretical calculation and atomic-scale characterization are strongly required for determination of the atomic and electronic structures at the interface, which play an important role in formation (carrier transport) of ohmic contacts to SiC.

Acknowledgements

The present work was partially supported by a grant-in-aid for Scientific Research on Priority Area, "Atomic Scale Modification (474)", from the Ministry of Education, Culture, Sports, Science, and Technology of Japan (No. 19053001).

REFERENCES

1) P. G. Neudeck: J. Electron. Mater. **24** (1995) 283.
2) R. J. Trew: Phys. Status Solidi A **162** (1997) 409.
3) A. Itoh and H. Matsunami: Crit. Rev. Solid State Mater. Sci. **22** (1997) 111–197.
4) R. R. Siergiej, R. C. Clarke, S. Sriram, A. K. Agarwal, R. J. Bojko, A. W. Morse, V. Balakrishna, M. F. MacMillan, A. A. Burk, Jr. and C. D. Brandt: Mater. Sci. Eng. B **61–62** (1999) 9.
5) R. J. Trew, J. B. Yan and P. M. Mock: Proc. IEEE **79** (1991) 598.
6) R. F. Davis, G. Kelner, M. Shur, J. W. Palmour and J. A. Edmond: Proc. IEEE **79** (1991) 677.
7) J. Crofton, P. A. Barnes, J. R. Williams and J. A. Edmond: Appl. Phys. Lett. **62** (1993) 384.
8) J. Crofton, L. Beyer, J. R. Williams, E. D. Luckowski, S. E. Mohney and J. M. Delucca: Solid-State Electron. **41** (1997) 1725.
9) S. Tanimoto, N. Kiritani, M. Hoshi and H. Okushi: Mater. Sci. Forum **389–393** (2002) 879.
10) J. Crofton, S. E. Mohney, J. R. Williams and T. Isaacs-Smith: Solid-State Electron. **46** (2002) 109.
11) S. E. Mohney, B. A. Hull, J. Y. Lin and J. Crofton: Solid-State Electron. **46** (2002) 689.
12) O. Nakatsuka, T. Takei, Y. Koide and M. Murakami: Mater. Trans. **43** (2002) 1684–1688.
13) B. J. Johnson and M. A. Capano: Solid-State Electron. **47** (2003) 1437.
14) S. Tsukimoto, K. Nitta, T. Sakai, M. Moriyama and M. Murakami: J. Electon. Mater. **33** (2004) 460.
15) T. Sakai, K. Nitta, S. Tsukimoto, M. Moriyama and M. Murakami: J. Appl. Phys. **95** (2004) 2187.
16) B. Pécz, L. Tóth, M. di Forte-Poisson and J. Vacas: Appl. Surf. Sci. **206** (2003) 8.
17) B. J. Johnson and M. A. Capano: J. Appl. Phys. **95** (2004) 5616.
18) J. Y. Lin, S. E. Mohney, M. Smalley, J. Crofton, J. R. Williams and T. I. Smith: 2000 Fall Meeting Proc. Silicon Carbide-Materials, ed. by A. K. Agarwal, J. A. Cooper, Jr., E. Janzen and M. Skowronski (Materials Research Society, Warrendale, PA, 2000) p. 640.
19) J. C. Viala, N. Peillon, F. Bosselet and J. Bouoix: Mater. Sci. Eng. A **229** (1997) 95.
20) JCPDS-ICDD PDF No. 22-1317.
21) T. Goto and T. Hirai: Mater. Res. Bull. **22** (1987) 1195. (JCPDS-ICDD PDF No. 40-1132)
22) T. Kimoto, A. Itoh and H. Matsunami: J. Appl. Phys. **81** (1997) 3494–3500.